sustainability

MDPI

Article

Suitability Evaluation of a Train's Scheduled Section Travel Time

Maosheng Li, Qing Huang *, Lixuan Yao and Yongliang Wang

School of traffic and transportation engineering, Central South University, Changsha 410083, China; maosheng.li@csu.edu.cn (M.L.); yaolixuan6093@163.com (L.Y.); pittylw@163.com (Y.W.)

* Correspondence: huangqing37@csu.edu.cn; Tel.: +86-1527-484-1386

Received: 2 March 2020; Accepted: 16 March 2020; Published: 19 March 2020

Abstract: Two methods used to evaluate the suitability of a train's scheduled section travel time (TSSTT) are theoretical modeling and data analysis. The first is suitable for newly constructed railway projects, the second can reveal the reliability of the train section running time (TSRT) under an instruction of TSSTT in cases where the train operation data are provided. A suitability evaluation method of TSSTT is proposed by calculating the possibility that a train completes a task within the time windows, centering on the TSSTT given in advance. The TSRTs between two adjacent stations are classified into four groups based on whether the train dwells at the two end stations of the railway section, and then subdivided secondly into subgroups by the instruction of TSSTT given. The kurtosis of each subgroup data of TSRT is larger than 3, so Weibull distribution is selected to fit the TSRT distribution of subgroup data due to good fitness based on root measurement of the least square (SRLSM). A busy high-speed railway line in the Wuhan area of China is used to validate the presented approach. Each railway section has its own suitable TSSTT in which TSRT might achieve 96% reliability of arriving within 2.5 minutes centering on suitable TSSTT, otherwise which might not obtain 10% reliability.

Keywords: suitability; reliability; train's scheduled section travel time; train section running time

1. Introduction

A working diagram of railway system specifies wagon routing, start time, and time consumption of each train at each component of railway network, and it also gives trains' scheduled section travel time (TSSTT) between two adjacent stations and dwelling time at each station. The actual train actual section running time (TSRT) and dwelling time in stations are affected by various factors, such as weather, power supply, train passenger capacity, passenger organization mode, train control system, and even the working diagram itself. Revealing the time deviation between TSRT and TSSTT on the railway section between two adjacent stations is the basis for compiling a highly reliable working diagram for the trains. Many factors affect TSSTT. First, the technical conditions of the railway line regarding safety constraints, such as the train's section speed limitations, should be met [1–9]. Additionally, the requirements of network operation and various passengers demand should be satisfied [10–15]. Lastly, energy conservation and environmental protection should be considered [16–21]. Hence, TSSTT should not only meet the demands of compiling a working diagram at the network level under different passenger needs, but also should consider energy conservation and environmental protection while ensuring that the TSRT on the same railway section falls within the neighborhood of TSSTT. The railway dispatching command system and operation-monitoring system can not only provide the scheduled arrival and departure time of a train at each working station but also precisely record actual arrival and departure time of a train at each working station. Hence, there are enough data needed to judge the suitability of TSSTT and any deviation between TSRT and TSSTT as a result of different factors,

such as the weather, power, carrying capacity, and train-operation control. At present, due to the lack of appropriate analysis tools, a mass of recorded data cannot be converted to valuable information for management purposes. On the other hand, the relevant departments of the railway operating company lack scientific and quantitative information for compiling train working diagrams which, instead, rely on traction-based simulation or subjective experience.

TSRT based on traction calculation is determined by equations of motion combined with the relationship between train tractive and braking forces, the sum of mechanical and aerodynamic resistances, and force caused by the track gradient, which reflect the train's section traction, idling, and brake operation process [16–19]. Hence, noise factors such as weather and power supply [9] on the railway line are considered less in the calculation process.

Multiple noise factors can cause an actual train's running time to deviate from the planned travel time and destroy the schedule, even causing delay propagation that affects passenger service. Suitable approaches for the detailed statistical analysis of train delays and validation of running and dwell times based on standard track occupation and release data, including goodness-of-fit test and estimates for the distributions and their parameters, have been provided in some articles [22,23]. Existing studies assume that train delays are subject to negative exponential distribution [5,11,12,24,25]. The frequency distribution of trains behind the schedule is subject to negative exponential distribution. The total number of trains, number of late train trips, and total time of trains behind schedule can be surveyed at a station or railway section. Hence, the average headway time of trains behind schedule is calculated from the total time of trains behind schedule divided the number of late train trips. The buffer time of a train can then be calculated by the negative exponential distribution [11,23,26] or weighted exponential distribution [27]. This is a conservative method with some deficits, such as the following. First, the method of calculating buffer time depends only on headway time of trains behind the schedule, which does not consider the proportion of trains behind schedule. In cases where the possibility of late trains is very small, the method may waste railway line capacity by inserting buffer time into schedule with very small chance of delays. Second, train delays are caused by weather, electricity supply, train capacity, passenger organization, train-operation control, the train working diagram, and other reasons, but the negative exponential distribution of delaying trains does not reveal relationship between late arrivals and causes of delays, and parameters of negative exponential distribution must be reevaluated after adjusting trains' working diagram. These parameters are not stable, which causes uncertainty in trains' working diagram.

There are also a lot of efforts on obtaining the distribution of TSRTs in order to incorporate knock-on delays in the modeling of delay propagation in network [27–31]. Many data resources such as train describer, track occupation, and clearance records are used for this purpose. A group of candidate distributions such as normal distribution, Weibull distribution, gamma distribution, and beta distribution are considered to fit the empirical data. These efforts do not distinguish the railway systematic and stochastic factors on train delays, so they cannot reveal the relationship between factors and train delays. In actuality, delays that happen on the upstream railway sections and stations may be not relevant to the train running time of the downstream railway sections and can be excluded in data preprocessing. Nowadays, there are two different research directions: many studies focus on how delays are propagated in heavy busy railway systems [27–31], but few pay attention to how to shorten the headway time among successive trains on railway line or route conflict junction, ensuring reliability of the trains' working diagram on the railway system with a relatively high level of punctuality and recovery from train delays to some extent.

In this paper, railway section refers to the railway line section between two adjacent stations, each of which might be working station for some trains, and the section might include more than one block section or other technical sections. TSRT can be calculated from the train arrival time at its destination station minus the train departure time at the starting station, so TSRT excludes the propagation delays on upstream railway sections and the starting station while taking into account effects caused by weather, electricity supply, train capacity, passenger organization, train-operation

control, the train working diagram, and other reasons. TSRTs are classified into four groups based on whether train dwells on the two end stations of the railway section, and they are then subdivided into subgroups by the instruction of TSSTT given before train departs. The kurtosis of each subgroup data of TSRT are larger than 3, so rather than log-normal, normal distribution, gamma distribution or beta distribution, Weibull distribution is selected to fit the TSRT distribution due to good fitness based on root measurement of the least square. The new approach has obtained the conditional distributions of TSRT in the case of TSSTT, which benefits the reliability calculation of TSSTT in simplicity and effectiveness. On the basis of the study of the distribution of TSRT under different TSSTTs, this paper studies the suitable TSSTT for each railway section, considering the possibility of delays and accommodating robustness of train travel times. Parameters of theoretical distribution of TSRT are stable and are not relevant to the train's working diagram.

The remainder of this paper is organized as follows. The suitable travel time and criteria for measuring the reliability of train operations are given in Section 2. Section 3 provides the data description, which deals with selection of fitting functions, and distribution fitting process of TSRT is given in Section 4. The appropriate TSSTT for each railway section on the studied railway system is given in Section 5. The paper concludes in Section 6 with problems requiring further study.

2. Evaluation Criterion

Assume that the analyzed railway system is represented by a set of stations N. The directional railway section between any two stations in N is indicated by a, and the set of railway section a is denoted by A. The TSSTT set of all trains in section a is denoted by T_a, and arbitrary TSSTT t_i^a belongs to T_a (i.e., $t_i^a \in T_a$), where i represents the i^{th} scheduled section travel time on section a. In railway section a, the TSRT $\widetilde{t}_i^a$ is a random variable whose distribution is the conditional probability distribution of the TSSTT t_i^a. The probability density function of the distribution is assumed to be $\rho(\widetilde{t}_i^a t_i^a)$.

Train is running continuously in the railway section and might have jumped some stations. According to whether a train dwells or not, the natural railway section between two adjacent stations can be divided into four types by the notation (*,*). The asterisks in this notation can take the values 1 and 2, where 1 means the train passes the track section of relevant station and does not stop, and 2 indicates that the train stops at station. The four types of railway sections are (2,2), (1,2), (2,1), and (1, 1).

TSRTs are classified into four groups based on train's dwelling type on two end stations of the railway section, and then they are subdivided secondly into subgroups by the instruction of TSSTT given to the train driver. Although trains can be distinguished by its types further, TSRT are classified only based on two factors mentioned above for concision in the paper. The kurtosis of each subgroup data of TSRT are larger than 3, so rather than log-normal or normal distribution, Weibull distribution is selected to fit distribution of subgroup data of TSRT due to good fitness based on root measurement of the least square (SRLSM).

a. Suitability measurement

Assume that $\overline{c}, \underline{c}$ are two positive values, the probability $\int_{t_i^a-\underline{c}}^{t_i^a+\overline{c}} \rho(tt_i^a)dt$ of TSRT $\widetilde{t}_i^a$ on time interval $\left[t_i^a-\underline{c}, t_i^a+\overline{c}\right]$ centering on TSSTT t_i^a can be used to measure the suitability of TSSTT t_i^a. If the probability is greater than a given threshold β, the TSSTT t_i^a is appropriate.

b. Reliability measurement

Similarly, the probability $\int_{t_i^a-\underline{c}}^{t_i^a+\overline{c}} \rho(tt_i^a)dt$ of TSRT $\widetilde{t}_i^a$ within the time interval $\left[t_i^a-\underline{c}, t_i^a+\overline{c}\right]$ centering on TSSTT t_i^a can also be used to measure the reliability of the train operation. There are three purposes for studying the reliability of train operation. The first is to judge the reliability of the existing train working diagram; the second is to improve the reliability of the existing train working diagram by inserting a buffer time or dwell time supplements; and the third is to measure the ability of the control

system to realize the schedule in different running environments. In general, a train's working diagram requires a certain degree of reliability, which may be assumed as a given threshold α, $0 < \alpha < 1$. It is often required to solve $\bar{c}$ in Equation (1) to determine the buffer time or the supplements between trains in succession.

$$\int_{-\infty}^{t_i^a + \bar{c}} \rho(tt_i^a) dt = \alpha \quad (1)$$

3. Data Description

The used raw data were recorded by the pressure sensor of a track circuit from January 1 to March 30, 2016, from the Beijing–Shenzhen high-speed railway line in Wuhan railway administrative area (East Xuchang to North Chibi), as shown in Table 1. These data include destination code, station number, scheduled arrival and departure times, and actual arrival and departure times. On the basis of these records, we can calculate each train's TSSTT and TSRT as well as scheduled and actual dwelling time of train at station. The railway line in Wuhan railway administrative area starts at 780 kilometers and 712 meters and ends at 1353 kilometers and 654 meters from the Beijing west railway station, and the total length is 572.942 km. The northernmost station reaches East Xuchang station in Zhengzhou administrative area, and the southernmost station is East Yueyang Station in Guangzhou Railway Group. A total of 10 stations and one block post include West Luohe, West Zhumadian, East Minggang, East Xinyang, North Xiaogan, East Hengdian, L1L2 block post, Wuhan Gaosuchang, East Wulongquan, North Xianning, and North Chibi. East Wulongquan is the cross station, and the rest of the stations are passenger stations. The down direction is from West Luohe Railway Station to North Chibi Station; the opposite is the up direction. For the railway section from North Chibi to North Xianning, the train G80 passed North Chibi at 15:50:00, precisely at the scheduled time on March 12, 2016, and spent 12 minutes covering the distance from North Chibi to North Xianning. Arriving at North Xianning at 16:01:00, it was delayed by just 1 minute compared to the scheduled arrival time. Train G80 departed punctually at 16:03:00 from North Xianning for remaining trips as described in Table 1.

Raw data were recorded in the Wuhan railway administrative area, including high-speed trains and motor-train units in both the up and down directions, as long as trains passed through the area. Hence, the data show the following characteristics: trains either pass through all the stations within the area or run into the railway line from a station, or leave the railway line from a station. Table 2 shows the train-dwelling-station relationship table for some high-speed trains and a value of zero means the train does not pass through a station. For example, train G580 only passes through Wuhan Gaosuchang, L1L2 block post and East Hengdian, and only dwells at Wuhan Gaosuchang. There are 86 up-direction trains and 114 down-direction trains running in Wuhan railway administrative area. The number of motor-train units in the up and down directions is 31 and 22, respectively.

Table 1. Partial raw data.

	Station	Arrival Time	Departure Time	Arrival Trips	Departure Trips	Scheduled Arrival Time	Scheduled Departure Time
1	North Chibi	2016/3/12 Saturday 15:50:00	2016/3/12 Saturday 15:50:00	G80	G80	2016/3/12 Saturday 15:50:00	2016/3/12 Saturday 15:50:00
2	North Xianning	2016/3/12 Saturday 16:02:00	2016/3/12 Saturday 16:03:00	G80	G80	2016/3/12 Saturday 16:01:00	2016/3/12 Saturday 16:03:00
3	East Wulongquan	2016/3/12 Saturday 16:14:00	2016/3/12 Saturday 16:14:00	G80	G80	2016/3/12 Saturday 16:13:00	2016/3/12 Saturday 16:13:00
4	Wuhan Gaosuchang	2016/3/12 Saturday 16:27:00	2016/3/12 Saturday 16:32:00	G80	G80	2016/3/12 Saturday 16:28:00	2016/3/12 Saturday 16:33:00
5	L1L2 Block Post	2016/3/12 Saturday 16:37:00	2016/3/12 Saturday 16:37:00	G80	G80	2016/3/12 Saturday 16:38:00	2016/3/12 Saturday 16:38:00
6	East Xuchang	2016/3/12 Saturday 18:07:00	2016/3/12 Saturday 18:09:00	G80	G80	2016/3/12 Saturday 18:07:00	2016/3/12 Saturday 18:09:00
7	North Chibi	2016/3/11 Friday 15:49:00	2016/3/11 Friday 15:49:00	G80	G80	2016/3/11 Friday 15:50:00	2016/3/11 Friday 15:50:00
8	North Xianning	2016/3/11 Friday 16:01:00	2016/3/11 Friday 16:02:00	G80	G80	2016/3/11 Friday 16:01:00	2016/3/11 Friday 16:03:00
9	East Wulongquan	2016/3/11 Friday 16:12:00	2016/3/11 Friday 16:12:00	G80	G80	2016/3/11 Friday 16:13:00	2016/3/11 Friday 16:13:00
10	Wuhan Gaosuchang	2016/3/11 Friday 16:26:00	2016/3/11 Friday 16:31:00	G80	G80	2016/3/11 Friday 16:28:00	2016/3/11 Friday 16:33:00
11	L1L2 Block Post	2016/3/11 Friday 16:36:00	2016/3/11 Friday 16:36:00	G80	G80	2016/3/11 Friday 16:38:00	2016/3/11 Friday 16:38:00
12	East Xuchang	2016/3/11 Friday 18:07:00	2016/3/11 Friday 18:09:00	G80	G80	2016/3/11 Friday 18:07:00	2016/3/11 Friday 18:09:00

Table 2. Train-dwelling-station relationship table in the up direction.

Trips	North Chibi	North Xianning	East Wulongquan	Wuhan Gaosuchang	L1/L2 Block Post	East Hengdian	North Xiaogan	East Xinyang	East Minggang	West Zhumadian	West Luohe	East Xuchang
G554	0	0	0	2	1	1	1	2	2	2	1	0
G580	0	0	0	2	1	1	0	0	0	0	0	0
G546	0	0	0	2	1	1	1	2	2	2	1	2
G544	0	0	0	2	1	1	1	2	1	2	2	1

The total number of track circuit records is 91,080 items, which includes 9109 items on the section between North Xianning and North Chibi; other information on each section is listed in Table 3.

Table 3. Characteristic values of train section running time (TSRT) in the down direction for all sections.

Section	Type	Schedule Time (min)	Min $\tilde{t}^{k}$ (s)	Max $\tilde{t}^{k}$ (s)	Range	Average (s)	*Standard Deviation*	Skewness	Kurtosis
North Chibi–North Xianning	(2,2)	13	13	25	12	14.63	1.61	4.91	31.66
		14	14	18	4	14.75	0.83	1.31	5.08
	(2,1)	10	11	13	2	11.44	0.56	0.72	2.43
		11	11	16	5	11.62	0.89	1.70	6.30
		13	11	16	5	11.63	0.83	2.62	14.20
	(1,1)	8	8	43	35	9.05	1.74	13.70	263.56
		9	8	15	7	9.12	1.04	1.45	5.82
		10	8	22	14	9.32	1.23	3.85	32.86
	(1,2)	11	11	17	6	12.41	1.13	1.55	5.94
		12	10	16	6	12.49	1.01	1.23	4.61
Wuhan Gaosuchang–L1L2 Block Post	(2,1)	5	4	25	21	5.39	0.86	6.36	111.13
		6	4	7	3	5.08	0.43	0.64	5.97
	(1,1)	5	4	13	9	5.70	0.69	1.89	15.76
L1L2 Block Post–East Hengdian	(1,1)	3	3	10	7	3.94	1.09	2.60	12.36
		4	3	25	22	3.81	0.91	5.74	104.26
		5	4	8	4	4.85	0.48	0.025	6.58
East Hengdian–North Xiaogan	(1,1)	18	17	43	26	18.23	1.54	6.23	57.45
		19	18	27	9	20.02	1.43	2.22	12.00
	(1,2)	21	20	32	12	21.96	1.16	4.78	39.29
		22	21	31	10	22.50	1.46	3.38	20.52
North Xiaogan–East Xinyang	(2,2)	18	18	27	9	19.12	1.02	2.98	20.80
	(2,2)	15	15	36	21	15.65	2.06	8.24	80.04
		18	18	25	7	18.86	1.02	3.82	24.05
	(1,1)	13	12	34	22	12.93	1.41	7.94	101.72
		18	12	24	12	13.13	1.66	4.84	31.80
	(1,2)	16	15	40	25	16.66	1.49	7.06	85.55
		17	15	27	12	17.07	1.54	3.34	19.05
East Xinyang–East Minggang	(2,2)	13	13	19	6	14.07	0.72	2.65	16.34
		14	14	19	5	14.82	0.76	2.57	15.89
	(2,2)	10	10	15	5	10.80	0.62	2.33	18.06
		11	10	17	7	11.07	1.02	3.95	21.02
	(1,1)	8	7	16	9	8.01	0.77	5.17	41.73
		10	11	15	4	11.70	0.99	2.23	8.44
	(1,2)	13	14	16	2	15.05	0.73	-0.08	1.91
East Minggang–West Zhumadian	(2,2)	17	16	25	9	18.02	0.88	4.07	32.25
		18	17	25	8	18.52	1.01	4.29	28.86
	(2,1)	14	14	23	9	14.72	1.06	5.45	42.60
	(1,1)	12	10	26	16	11.90	1.32	5.78	45.25
		13	11	20	9	11.58	0.87	5.39	51.25
		14	11	20	9	11.67	1.20	5.62	39.79
	(1,2)	15	13	26	13	15.33	1.09	4.03	27.71
		16	15	22	7	15.72	0.98	4.45	29.80
West Zhumadian–West Luohe	(2,2)	18	15	27	12	19.12	1.14	3.08	17.23
		19	18	19	1	18.63	0.49	-0.55	1.31
		21	18	24	6	18.88	1.06	2.91	13.81
	(2,1)	15	13	25	12	15.72	1.42	3.96	22.40
		16	15	24	9	15.64	1.34	4.14	23.24
		18	15	24	9	15.60	1.38	4.20	24.17
		19	18	41	23	19.29	2.95	6.93	51.61
	(1,1)	13	10	25	15	13.06	1.52	5.05	34.27
		14	11	23	12	13.10	1.52	4.44	27.60
		17	13	18	5	16.33	0.82	-2.00	10.07
	(1,2)	16	14	27	13	16.60	1.52	3.72	20.89

Table 3. *Cont.*

Section	Type	Schedule Time (min)	Min $\tilde{t}^{k}$ (s)	Max $\tilde{t}^{k}$ (s)	Range	Average (s)	*Standard Deviation*	Skewness	Kurtosis
West Luohe–East Xuchang	(2,2)	16	11	22	11	16.39	1.20	-0.07	9.01
		17	13	23	10	16.94	1.07	0.46	8.86
		19	16	21	5	17.34	0.65	2.10	11.41
	(2,1)	13	10	21	11	13.49	1.18	2.73	15.91
		15	10	20	10	13.96	1.12	1.84	10.84
		16	10	19	9	13.95	1.24	1.51	8.37
	(1,1)	11	7	20	13	10.86	1.23	3.36	23.73
		13	8	20	12	11.09	0.99	4.66	40.26
		15	10	18	8	11.48	1.10	3.37	20.15
	(1,2)	14	10	22	12	14.20	1.34	2.14	15.20
		15	11	21	10	14.25	1.34	3.15	16.78
		17	14	23	9	15.89	1.58	2.53	10.87

4. Fitting Distribution of Train Running Time

It is helpful to determine a fitting function reflecting the distribution law of TSRT, which might benefit in optimizing a train's working diagram and historical data storage of TSRT. For fitting purposes, the maximum number, minimum value, distribution range, mean value, standard deviation, skewness, and kurtosis of TSRT are calculated according to each of the four section types, as shown in Table 3. As section lengths differ between different adjacent stations, the average section running times ("expected" column of Table 3) are not the same, but variances of TSRT are less than 2 ("standard deviation" column in Table 3), which means that high-speed trains have strong traction power and a highly reliable train-operation control system. It is evident from the range of TSRTs ("range" column in Table 3) that the gap is greater than 2 minutes, and up to 35 minutes, even in the same section and for the same TSSTT. This indicates that the ability of the train-operation control system to achieve the scheduled travel time must be improved and the current train's working diagram has great potential for optimization. The kurtosis values (last column of Table 3) are almost all greater than 3 except for three instances (row 4, 35 and 45), which indicates that the kurtosis of TSRT is stable. This character is different from urban metro trains, as shown in Table 3 of Li, Liu, et al. [32]. Hence, we can choose Weibull distribution with kurtosis greater than 3 to fit distribution of TSRT. As most of variances of TSRT are less than 2, whereas sometimes the values of range are quite large, there are some singular values in the data of TSRT. Due to the frequency of singular values of TSRT being very low, they are within 1.3% quantile and outside 98.5% quantile of data of TSRT. The total number of singular values is 3% of TSRT data. After the singular values are removed, Weibull distribution is used to fit data of TSRT. The least squares between frequency on the histogram of TSRT and probability of the fitting distribution are calculated, and SRLSM is set as a criterion to judge whether the fitting distribution is suitable. A signification test was executed and found that Weibull distribution fits data of TSRT on each section, but lognormal and normal distribution are partially fitted in some sections. Parameters of the fitting function and its value of SRLSM for West Luohe–East Xuchang are shown in Table 4. The table shows that the Weibull distribution is superior to the normal distribution and lognormal distribution.

Table 4. Parameters of the distribution function of TSRT of West Luohe–East Xuchang.

Section	Dwelling Type	%	Time	Lognormal Distribution			Normal Distribution			Weibull Distribution		
				1th Parameter	2th Parameter	SRLSM	1th Parameter	2th Parameter	SRLSM	1th Parameter	2th Parameter	SRLSM
West Luohe-East Xuchang	(1,1)	0.03	11	2.3700	0.0688	0.4864	10.7225	0.7596	0.4619	11.0943	8.0244	0.4937
		0.05	13	2.3957	0.0426	0.5023	10.9862	0.4663	0.4871	11.2102	22.9762	0.4035
		0.03	15	2.4270	0.0587	0.2823	11.3438	0.6719	0.2706	11.6679	16.5326	0.2385
	(1,2)	0.07	14	2.6492	0.0415	0.3581	14.1552	0.5941	0.3469	14.4509	19.3307	0.3321
		0.07	15	2.6404	0.0380	0.4224	14.0282	0.5319	0.4092	14.2857	26.7533	0.3281
		0.08	17	2.7421	0.0527	0.2311	15.5410	0.8281	0.2275	15.9460	18.9575	0.2471
	(2,1)	0.06	13	2.5881	0.0433	0.3397	13.3172	0.5742	0.3360	13.5899	26.5844	0.3148
		0.04	15	2.6276	0.0540	0.2341	13.8605	0.7595	0.2197	14.2346	17.1068	0.1882
		0.10	16	2.6266	0.0526	0.2582	13.8459	0.7389	0.2427	14.2119	17.1762	0.2066
	(2,2)	0.03	16	2.7944	0.0544	0.3563	16.3769	0.8666	0.3477	16.7550	24.0068	0.3068
		0.06	17	2.8268	0.0448	0.3969	16.9072	0.7439	0.3845	17.2429	26.9996	0.2959
		0.05	19	2.8503	0.0263	0.3415	17.2990	0.4602	0.3410	17.5377	36.6633	0.3272

5. Suitability of TSSTT

Set the high-speed railway station set as N = {East Xuchang, West Luohe, West Zhumadian, East Minggang, East Xinyang, North Xiaogan, East Hengdian, L1L2 block post, Wuhan Gaosuchang, East Wulongquan, North Xianning, North Chibi}, the research scope is from North Chibi station to East Xuchang station. Let a represent the West Luohe–East Xuchang section. Figure 1 shows the frequency of TSSTTs used for the trains' working diagram on West Luohe–East Xuchang section which is type (2,2) section. Noting that data are only accurate to the minute, the figure shows that the set of TSSTTs on type (2,2) section a is $T_a = \{16, 17, 18, 19, 20, 21, 22, 23, 24, 26, 27\}$. This demonstrates a variety of demand for TSSTT in the West Luohe–East Xuchang section. In three months, 16 minutes of TSSTT has appeared 468 times in total, which accounts for 48.1%, the highest frequency of occurrence. The next is 17 minutes which occurs 310 times, accounting for 31.9%. TSSTTs of 24, 26, and 27 minutes are used once, each accounting for 0.1% of the total number. Because TSSTTs greater than or equal to 20 minutes are less, the histograms of TSRTs and the fitted distributions are only plotted for 16–19 minutes, as shown in Figures 2–5, and the probability density function fitted is described as $\rho(\widetilde{t}_i^a t_i^a)$. For example, the graph in Figure 2 corresponds to TSSTT $t_1^a = 16$ minutes, and its probability density function is written as $\rho(\widetilde{t}_1^a 16)$. Other TSSTTs have similar usage and distribution rules.

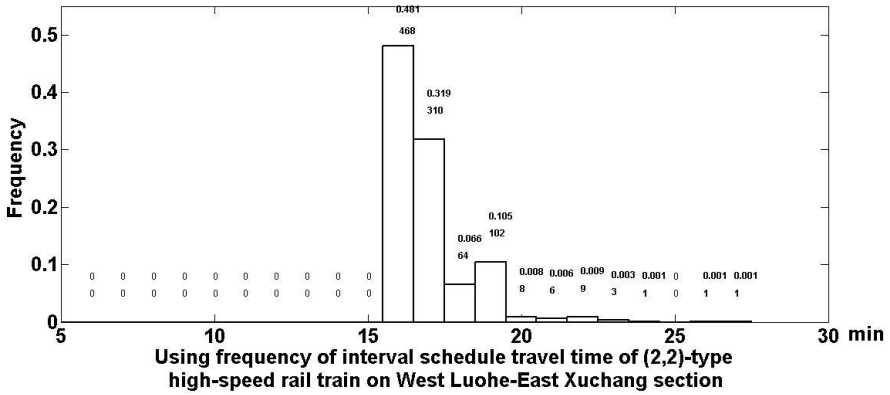

Figure 1. Frequency of train scheduled section travel times (TSSTTs) of a (2,2)-type high-speed rail train on West Luohe–East Xuchang section.

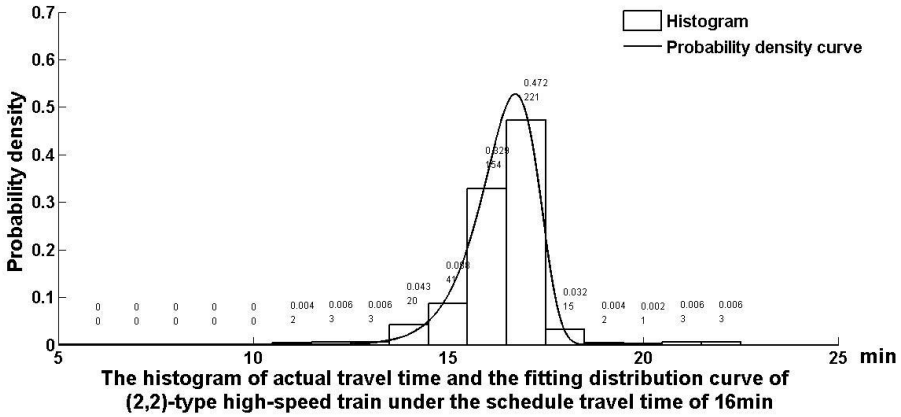

Figure 2. Histogram of train section running times (TSRTs) and the fitting distribution curve of a (2,2)-type high-speed train under the TSSTT of 16 minutes.

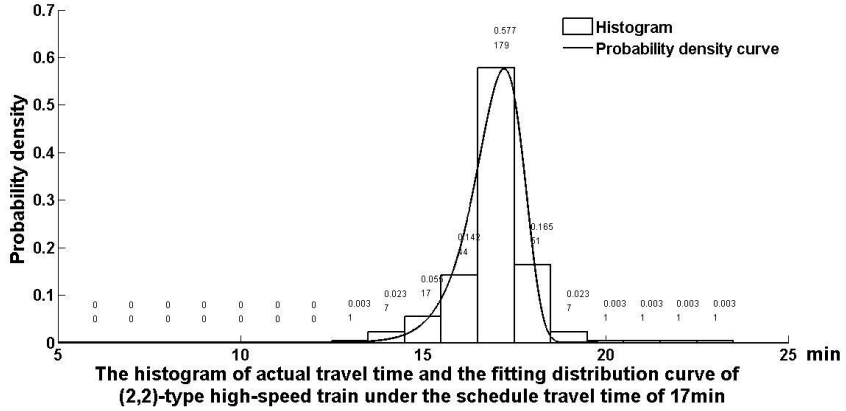

Figure 3. Histogram of TSRT and the fitting distribution curve of a (2,2)-type high-speed train under the TSSTT of 17 minutes.

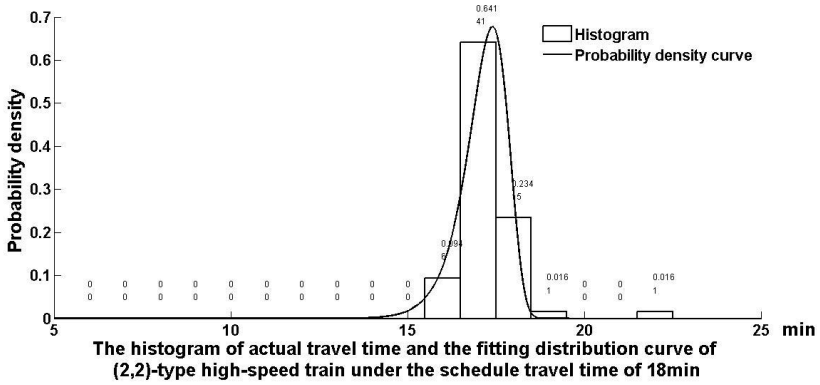

Figure 4. Histogram of TSRT and the fitting distribution curve of a (2, 2)-type high-speed train under the TSSTT of 18 minutes.

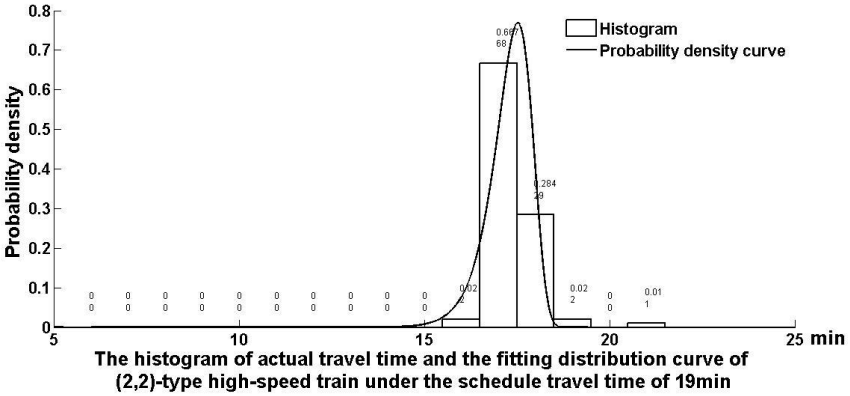

Figure 5. Histogram of TSRT and the fitting distribution curve of a (2,2)-type high-speed train under the TSSTT of 19 minutes.

Considering the accuracy of the statistical data is 1 minute, $\left(\bar{c}, \underline{c}\right)$ can be taken here to be (0.5,0.5), (1.5,1.5) and (2.5,2.5), respectively. According to Figure 2, the West Luohe–East Xuchang section of the schedule time accounts for 16 minutes, and $\left(\bar{c}, \underline{c}\right)$ is taken to be (0.5,0.5), (1.5,1.5), (2.5,2.5), probabilities of a punctual departure or arrival in the time zone $\left(16-\underline{c}, 16+\bar{c}\right)$ of a (2, 2)-type high-speed train are, respectively, as follows:

$$\int_{16-0.5}^{16+0.5} \rho(t16)dt = 0.329 \tag{2}$$

$$\int_{16-1.5}^{16+1.5} \rho(t16)dt = 0.889 \tag{3}$$

$$\int_{16-1.5}^{16+1.5} \rho(t16)dt = 0.889 \tag{4}$$

Similarly, according to Figures 3–5, we can calculate possibility of punctual departures and arrivals in the time zone $\left(t_i^a-\underline{c}, t_i^a+\bar{c}\right)$ of a (2, 2)-type train for different TSSTTs. They are shown in Table 5 for TSSTTs of 17, 18 and 19 minutes. Although $\left(\underline{c}, \bar{c}\right)$ is taken as (2.5, 2.5), possibility of a punctual departure or arrival in the time zone $\left(t_i^a-\underline{c}, t_i^a+\bar{c}\right)$ of a (2, 2)-type high-speed train is not much different from TSSTT of 16 and 17 minutes. Taking $\left(\bar{c}, \underline{c}\right)$ as (0.5, 0.5) and (1.5, 1.5) reveals that the possibility of a punctual departure or arrival in the time zone $\left(17-\underline{c}, 17+\bar{c}\right)$ will reach a maximum value, such as $\int_{17-0.5}^{17+0.5} \rho(t17)dt = 0.577$ and $\int_{17-1.5}^{17+1.5} \rho(t17) = 0.884$, respectively. There is $\int_{17-0.5}^{17+0.5} \rho(t17)dt = 0.577 > 0.329 = \int_{16-0.5}^{16+0.5} \rho(t16)dt$ and the possibility of a punctual departure or arrival in the time zone $(17-1.5, 17+1.5)$ is larger than the given threshold $\beta = 0.8$, namely $\int_{17-1.5}^{17+1.5} \rho(t17) = 0.884 > 0.8 = \beta$. These show that the schedule time for 17 minutes in the West Luohe–East Xuchang section is the most appropriate. Table 5 also gives the possibility of punctual departures and arrivals in the time zone $\left(t_i^a-\underline{c}, t_i^a+\bar{c}\right)$ of type (1, 2), (2, 1), and (1, 1) high-speed trains for different TSSTTs by the same calculation method. Table 6 shows the appropriate TSSTT value for each section in the Wuhan railway administrative area. As Table 5 shows, the reliability of TSRT can reach more than 96% in the neighborhood of 2.5 minutes centering on TSSTT. This reliability may be less than 10% under unsuitable TSSTT.

Table 5. Table of section travel time reliability.

Schedule Time (min)	Time Zone		Reliability of West Luohe–East Xuchang							
			(2,2)-Type		(2,1)-Type		(1,2)-Type		(1,1)-Type	
11	(11 − 0.5,11 + 0.5)	-	-		-		-		-	
	(11 − 1.5,11 + 1.5)	(111.5,11 + 0.5)	-	-	-	-	-	-	0.918	0.887
		(11 − 0.5,11 + 1.5)		-		-		-		0.696
	(11−2.5,11 + 2.5)	(11−2.5,11 + 0.5)	-	-	-	-	-	-	0.959	0.921
		(11−0.5,11 + 2.5)		-		-		-		0.703
12	(12 − 0.5,12 + 0.5)	-	-		-		-		-	
	(12 − 1.5,12 + 1.5)	(12 − 1.5,12 + 0.5)	-	-	-	-	-	-	0.83	0.779
		(12 − 0.5,12 + 1.5)		-		-		-		0.22
	(12 − 2.5,12 + 2.5)	(12 − 2.5,12 + 0.5)	-	-	-	-	-	-	0.983	0.915
		(12 − 0.5,12 + 2.5)		-		-		-		0.237
13	(13 − 0.5,13 + 0.5)	-	-		0.539		-		0.026	
	(13 − 1.5,13 + 1.5)	(13 − 1.5,13 + 0.5)	-		0.944	0.592	-	-	0.126	0.122
		(13 − 0.5,13 + 1.5)				0.891		-		0.03
	(13 − 2.5,13 + 2.5)	(13 − 2.5,13 + 0.5)	-		0.948	0.596	-	-	0.868	0.864
		(13 − 0.5,13 + 2.5)				0.891		-		0.03
14	(14 − 0.5,14 + 0.5)	-	-		0.541		0.612		0.146	
	(14 − 1.5,14 + 1.5)	(14 − 1.5,14 + 0.5)	-	-	0.935	0.918	0.895	0.693	0.5	0.396
		(14 − 0.5,14 + 1.5)		-		0.557		0.814		0.25
	(14 − 2.5,14 + 2.5)	(14 − 2.5,14 + 0.5)	-	-	0.95	0.934	0.948	0.724	0.771	0.646
		(14 − 0.5,14 + 2.5)		-		0.557		0.836		0.271
15	(15 − 0.5,15 + 0.5)	-	-		0.134		0.144		0	
	(15 − 1.5,15 + 1.5)	(15 − 1.5,15 + 0.5)	-	-	0.933	0.799	0.837	0.811	0.015	0.015
		(15 − 0.5,15 + 1.5)		-		0.609		0.17		0
	(15 − 2.5,15 + 2.5)	(15 − 2.5,15 + 0.5)	-	-	0.967	0.805	0.955	0.929	0.06	0.06
		(15 − 0.5,15 + 2.5)		-		0.637		0.17		0
16	(16 − 0.5,16 + 0.5)	-	0.329		0.028		-		-	
	(16 − 1.5,16 + 1.5)	(16 − 1.5,16 + 0.5)	0.889	0.417	0.157	0.136	-	-	-	-
		(16 − 0.5,16 + 1.5)		0.801		0.049		-		-
	(16 − 2.5,16 + 2.5)	(16 − 2.5,16 + 0.5)	0.964	0.46	0.643	0.619	-	-	-	-
		(16 − 0.5,16 + 2.5)		0.833		0.052		-		-
17	(17 − 0.5,17 + 0.5)	-	0.577		0.1		0.152		-	
	(17 − 1.5,17 + 1.5)	(17 − 1.5,17 + 0.5)	0.884	0.719	0.226	0.138	0.424	0.394	-	-
		(17 − 0.5,17 + 1.5)		0.742		0.126		0.182		-
	(17 − 2.5,17 + 2.5)	(17 − 2.5,17 + 0.5)	0.962	0.765	0.277	0.176	0.909	0.879	-	-
		(17 − 0.5,17 + 2.5)		0.774		0.201		0.182		-
18	(18 − 0.5,18 + 0.5)	-	0.234		0.127		-		-	
	(18 − 1.5,18 + 1.5)	(18 − 1.5,18 + 0.5)	0.891	0.875	0.451	0.423	-	-	-	-
		(18 − 0.5,18 + 1.5)		0.25		0.155		-		-
	(18 − 2.5,18 + 2.5)	(18 − 2.5,18 + 0.5)	0.985	0.969	0.662	0.634	-	-	-	-
		(18 − 0.5,18 + 2.5)		0.25		0.155		-		-
19	(19 − 0.5,19 + 0.5)	-	0.02		-		-		-	
	(19 − 1.5,19 + 1.5)	(19 − 1.5,19 + 0.5)	0.304	0.304	-	-	-	-	-	-
		(19 − 0.5,19 + 1.5)		0.02		-		-		-
	(19 − 2.5,19 + 2.5)	(19 − 2.5,19 + 0.5)	0.981	0.971	-	-	-	-	-	-
		(19 − 0.5,19 + 2.5)		0.03		-		-		-

Table 6. Suitable TSSTT for each section and train dwelling type.

Section	Train Dwelling Type	The Suitable TSSTT (min)
North Chibi–North Xianning	(2,2)	15
	(2,1)	11
	(1,2)	11
North Xianning–East Wulongquan	(1,1)	7
	(2,1)	9
East Wulongquan–Wuhan Gaosuchang	(1,1)	12
	(1,2)	13
Wuhan Gaosuchang–L1L2 Block Post	(1,1)	4
	(2,1)	6
L1L2 Block Post–East Hengdian	(1,1)	4
East Hengdian–North Xiaogan	(1,1)	18
	(1,2)	22
North Xiaogan–East Xinyang	(1,1)	13
	(1,2)	16
	(2,1)	15
	(2,2)	19
East Xinyang–East Minggang	(1,1)	8
	(1,2)	14
	(2,1)	11
	(2,2)	15
East Minggang–West Zhumadian	(1,1)	12
	(1,2)	15
	(2,1)	15
	(2,2)	18
West Zhumadian–West Luohe	(1,1)	13
	(1,2)	16
	(2,1)	15
	(2,2)	19
West Luohe–East Xuchang	(1,1)	11
	(1,2)	14
	(2,1)	13
	(2,2)	17

If a train lagged slightly, it may be asked to run speed up in order to recover the schedule time while ensuring safety, which is referred to a "hurry" task. To demonstrate the ability of the high-speed train to complete the "hurry" task, Table 5 shows the possibility that the train reaches the station on time when $\left(\underline{c}, \bar{c}\right)$ equals (1.5,0.5), (0.5,1.5), (2.5,0.5), and (0.5,2.5). For example, in the West Luohe–East Xuchang section, the possibility of a (2, 2)-type high-speed train departing or arriving punctually in the time zone $(16-1.5, 16+0.5)$, $(16-2.5, 16+0.5)$ is 0.417 and 0.460, respectively, which shows that the train is not able to complete a "hurry" task in the case of tight time due to the running speed not exceeding 300 km/h. The possibility of a (2, 2)-type train departing and arriving punctually in the time zone $(19-1.5, 19+0.5)$, $(19-2.5, 19+0.5)$ is 0.304 and 0.971, respectively. This means that the "hurry" task can be completed under the speed limit of 300 km/h in the same section when the scheduled travel time is 19 minutes. The performance differs according to the type of train on the same section. The performance gradually worse as the type changes in the following sequence: (2,2), (2,1), (1,2), (1,1).

Until now, the high-speed railway has operated from 6:00 a.m. to 10:00 p.m., 16 hours a day. A total of 127 high-speed trains and motor-train units run in the up direction, with an average headway time of 7.56 minutes. A total of 136 high-speed trains and motor-train units run in the down direction, with an average train gap time of 7.06 minutes. Hence, there are fewer knock-on delays among a cascade of high-speed trains, not like urban railway trains, whose running time distribution comply

with the rule of the censored model with shifting character [32]. Figures 2–5 show that the possibility of a train punctually reaching a station in the time window $\left(t_i^a - 3.5, t_i^a + 3.5\right)$ under an appropriate TSSTT t_i^a can reach more than 99%. In other words, the reliability of the high-speed train within the 7-minute headway time can reach 99% under the current passenger demand in Wuhan railway administrative area, even in a complex running environment.

6. Conclusions

We calculated that the kurtosis of TSRT is greater than 3 and is stable. The shifting character of a limited-variable model relative to TSRT of an urban subway train [32] does not appear on the high-speed railway system. The headway times between high-speed trains are relatively large, so delay propagation among trains rarely occur. This may be the main cause for the absence of the shifting character of TSRT of high-speed trains. Some results are as follows:

1. Passenger demand requires the availability of trains' working diagram with different TSSTT. Under different TSSTT instructions, the reliability of TSRT is different.
2. With factors including weather, electricity supply, train passenger capacity, passenger organization, train operation control, and line conditions, each section has an appropriate TSSTT. If the train working diagram uses the appropriate TSSTT, it is highly likely for trains to complete the task as planned.
3. The ability of trains to complete a "hurry" task can be assessed by reliability.
4. Weibull distribution can be used to fit the distribution of TSRT with different TSSTTs.

Forthcoming research will focus on how to use these new findings to improve the reliability of trains' working diagram, and a comprehensive comparison with different methods will be proceeded in near future

Author Contributions: Conceptualization, M.L.; methodology, M.L.; software, Y.W.; validation, Q.H., M.L. and L.Y.; formal analysis, L.Y. and Y.W.; data curation, L.Y., Q.H. and Y.W.; writing—original draft preparation, Q.H. and L.Y.; writing—review and editing, Q.H. and M.L. All authors have read and agreed to the published version of the manuscript.

Funding: This work was supported by the National Social Science Fund under grant number 14BJT017 and the Mathematics and Interdisciplinary Science Project of Central South University in 2014.

Acknowledgments: The authors send their appreciation to the Central South University and the National Social Science Fund.

Conflicts of Interest: The authors declare no conflicts of interest.

References

1. Higgins, A.; Kozan, E. Modeling train delays in urban networks. *Transp. Sci.* **1998**, *32*, 346–357. [CrossRef]
2. Chang, Y.H.; Yeh, C.H.; Shen, C.C. A multi-objective model for passenger train services planning: Application to Taiwan's high-speed rail line. *Transport. Res. B Meth.* **2000**, *34*, 91–106. [CrossRef]
3. Abril, M.; Barber, F.; Ingolotti, L.; Salido, M.; Tormos, P.; Lova, A. An assessment of railway capacity. *Transp. Res. Part E Logist. Transp. Rev.* **2008**, *44*, 774–806. [CrossRef]
4. Castillo, C.; Gallego, I.; Ureña, J.M.; Coronado, J.M. Timetabling optimization of a mixed double-and single-tracked railway network. *Appl. Math. Model.* **2011**, *35*, 859–878. [CrossRef]
5. Cacchiani, V.; Toth, P. Nominal and robust train timetabling problems. *Eur. J. Oper. Res.* **2012**, *219*, 727–737. [CrossRef]
6. Barrena, E.; Canca, D.; Coelho, L.C.; Laporte, G. Exact formulations and algorithm for the train timetabling problem with dynamic demand. *Comput. Oper. Res.* **2014**, *44*, 66–74. [CrossRef]
7. Jovanovic, P.; Kecman, P.; Bojović, N.J.; Mandić, D. Optimal allocation of buffer times to increase train schedule robustness. *Eur. J. Oper. Res.* **2017**, *256*, 44–54. [CrossRef]

8. Luan, X.; Miao, J.; Meng, L.; Corman, F.; Lodewijks, G. Integrated optimization on train scheduling and preventive maintenance time slots planning. *Transp. Res. Part C Emerg. Technol.* **2017**, *80*, 329–359. [CrossRef]
9. Song, Y.; Liu, Z.; Wang, H.; Zhang, J.; Lu, X.; Duan, F. Analysis of the galloping behaviour of an electrified railway overhead contact line using the non-linear finite element method. *Proc. Inst. Mech. Eng. Part F J. Rail Rapid Transit* **2018**, *232*, 2339–2352. [CrossRef]
10. Goossens, J.-W.; Van Hoesel, C.; Kroon, L. On solving multi-type railway line planning problems. *Eur. J. Oper. Res.* **2006**, *168*, 403–424. [CrossRef]
11. Vansteenwegen, P.; Van Oudheusden, D. Developing railway timetables which guarantee a better service. *Eur. J. Oper. Res.* **2006**, *173*, 337–350. [CrossRef]
12. Kroon, L.; Maroti, G.; Helmrich, M.R.; Vromans, M.; Dekker, R. Stochastic improvement of cyclic railway timetables. *Transp. Res. Part B Methodol.* **2008**, *42*, 553–570. [CrossRef]
13. Espinosa-Aranda, J.L.; Garcia-Rodenas, R.; Ramírez-Flores, M.D.C.; Lopez-Garcia, M.L.; Angulo, E. High-speed railway scheduling based on user preferences. *Eur. J. Oper. Res.* **2015**, *246*, 772–786. [CrossRef]
14. Yang, L.; Qi, J.; Li, S.; Gao, Y. Collaborative optimization for train scheduling and train stop planning on high-speed railways. *Omega* **2016**, *64*, 57–76. [CrossRef]
15. Guo, X.; Wu, J.; Zhou, J.; Yang, X.; Wu, D.; Gao, Z. First-train timing synchronisation using multi-objective optimisation in urban transit networks. *Int. J. Prod. Res.* **2018**, *57*, 3522–3537. [CrossRef]
16. Howlett, P.; Pudney, P.; Vu, X. Local energy minimization in optimal train control. *Automatica* **2009**, *45*, 2692–2698. [CrossRef]
17. Albrecht, A.; Howlett, P.; Pudney, P.; Vu, X. Energy-efficient train control: From local convexity to global optimization and uniqueness. *Automatica* **2013**, *49*, 3072–3078. [CrossRef]
18. Albrecht, A.; Howlett, P.; Pudney, P.; Vu, X.; Zhou, P. The key principles of optimal train control—Part 1: Formulation of the model, strategies of optimal type, evolutionary lines, location of optimal switching points. *Transp. Res. Part B Methodol.* **2016**, *94*, 482–508. [CrossRef]
19. Ye, H.; Liu, R. A multiphase optimal control method for multi-train control and scheduling on railway lines. *Transp. Res. Part B Methodol.* **2016**, *93*, 377–393. [CrossRef]
20. Huisman, T.; Boucherie, R.J. Running times on railway sections with heterogeneous train traffic. *Transp. Res. Part B Methodol.* **2001**, *35*, 271–292. [CrossRef]
21. Sun, H.; Wu, J.; Ma, H.; Yang, X.; Gao, Z. A Bi-objective timetable optimization model for urban rail transit based on the time-dependent passenger volume. *IEEE Trans. Intell. Transp. Syst.* **2018**, *20*, 604–615. [CrossRef]
22. Yuan, J.; Medeossi, G. Statistical analysis of train delays and movements. In *Railway Timetabling & Operations*; Hansen, I., Pachl, J., Eds.; DVV Media Group Eurail Press: Hamburg, Germany, 2014; pp. 217–236.
23. Kecman, P.; Goverde, R.M.P. Train delay prediction. In *Railway Timetabling & Operations*; Hansen, I., Pachl, J., Eds.; DVV Media Group Eurail Press: Hamburg, Germany, 2014; pp. 237–252.
24. Hu, S.J. *The Train Operation Organization and Capacity Theory*; China Railway Press: Beijing, China, 1993; pp. 101–162.
25. Bury, K. *Statistical Distributions in Engineering*; Cambridge University Press (CUP): Cambridge, UK, 1999; pp. 178–207.
26. Salido, M.; Barber, F.; Ingolotti, L. Robustness for a single railway line: Analytical and simulation methods. *Expert Syst. Appl.* **2012**, *39*, 13305–13327. [CrossRef]
27. Yuan, J.; Hansen, I.A. Closed form expressions of optimal buffer times between scheduled trains at railway bottlenecks. In Proceedings of the 2008 11th International IEEE Conference on Intelligent Transportation Systems, Beijing, China, 12–15 October 2008; pp. 675–680.
28. Goverde, R.M.P.; Hansen, I.A.; Hooghiemstra, G.; Lopuhaä, H.P. Delay distributions in railway stations. In Proceedings of the 9th World Conference on Transport Research, Seoul, Korea, 22–27 July 2001.
29. Yuan, J. *Stochastic Modelling of Train Delays and Delay Propagation in Stations*; Eburon Uitgeverij BV: Vredenburg, The Netherlands, 2006.
30. Flier, H.; Gelashvili, R.; Graffagnino, T.; Nunkesser, M. Mining railway delay dependencies in large-scale real-world delay data. In *Robust and Online Large-Scale Optimization: Models and Techniques for Transportation Systems*; Ahuja, R.K., Möhring, R.H., Zaroliagis, C.D., Eds.; Springer: Berlin, Germany, 2009; pp. 354–368.
31. Hansen, I.A.; Goverde, R.; Van Der Meer, D.J. Online train delay recognition and running time prediction. In Proceedings of the 13th International IEEE Conference on Intelligent Transportation Systems, Funchal, Portugal, 19–22 September 2010; pp. 1783–1788.

32. Li, M.-S.; Liu, Z.; Zhang, Y.; Liu, W.; Shi, F. Distribution analysis of train interval journey time employing the censored model with shifting character. *J. Appl. Stat.* **2016**, *44*, 1–19. [CrossRef]